

# Fractional power-law conductivity in $\text{SrRuO}_3$ and its consequences

J. S. Dodge,<sup>1,2</sup> C. P. Weber,<sup>1,2</sup> J. Corson,<sup>1,2</sup> J. Orenstein,<sup>1,2</sup> Z. Schlesinger,<sup>3</sup> J. W. Reiner,<sup>4</sup> and M. R. Beasley<sup>4</sup>

<sup>1</sup>*Department of Physics, University of California at Berkeley, Berkeley, California 94720*

<sup>2</sup>*Materials Sciences Division, E. O. Lawrence Berkeley National Laboratory, Berkeley, California 94720*

<sup>3</sup>*Department of Physics, University of California at Santa Cruz, Santa Cruz, California 95064*

<sup>4</sup>*Edward L. Ginzton Laboratories, Stanford University, Stanford, California 94305*

(Dated: November 3, 2018)

We combine the results of terahertz time-domain spectroscopy with far-infrared transmission and reflectivity to obtain the conductivity of  $\text{SrRuO}_3$  over an unprecedented continuous range in frequency, allowing us to characterize the approach to zero frequency as a function of temperature. We show that the conductivity follows a simple phenomenological form, with an analytic structure fundamentally different from that predicted by the standard theory of metals.

PACS numbers: 72.15.Qm, 78.66.Bz, 75.20.En, 74.20.Mn

One of the most exciting proposals to emerge from the study of high- $T_c$  superconductors is that Landau's Fermi liquid theory (FLT) breaks down in the metallic state above  $T_c$  [1]. This would have profound implications, since FLT provides the foundation for our current understanding of metals, together with systems as diverse as liquid  $^3\text{He}$  and nuclear matter [2]. Evidence for its breakdown in high- $T_c$  superconductors comes from a variety of experiments, including photoemission, electrical transport and optics [3]. More recently similar evidence has been found in other compounds [4]. Here we show that the complex optical conductivity  $\sigma(\omega, T)$  of one such material, the ferromagnetic metal  $\text{SrRuO}_3$  [5, 6, 7, 8], behaves according to a remarkably simple power-law form, which deviates sharply from the prediction of FLT. This observation provides valuable insight into the nature of charge scattering in unconventional metals.

According to FLT, the qualitative properties of an interacting electron gas are the same as those of a non-interacting gas, if probed on a sufficiently low-energy scale. The optical conductivity of a system of noninteracting, charge  $e$  carriers obeys the Drude form,  $\sigma(\omega) = (ne^2/m)/(1/\tau - i\omega)$ , where  $n$  is the carrier density and  $m$  and  $\tau$  are the effective mass and scattering time of the carriers. FLT predicts that  $\sigma$  at low  $\omega$  remains of the Drude form in the presence of interactions, with a spectral weight which decreases as interactions increase. The  $f$ -sum rule dictates that the total spectral weight is conserved, so that spectral weight must shift to higher energies. This additional component to  $\sigma(\omega)$  is known as the incoherent part of the intraband conductivity.

Infrared reflectivity studies indicate that both high- $T_c$  superconductors and  $\text{SrRuO}_3$  exhibit conductivity with an anomalous power-law dependence on frequency,  $\sigma_1(\omega) \propto \omega^{-\alpha}$ , with  $\alpha \sim 0.5$  for  $\text{SrRuO}_3$  [8] and  $\alpha \sim 0.7$  in the high- $T_c$  materials [9, 10]. The Drude form yields  $\sigma_1 \propto \omega^{-2}$  at comparable frequencies. If FLT is valid, the conductivity in excess of Drude must be identified with interband transitions or the incoherent component of the spectrum, and there must be a crossover at lower fre-

quency to the renormalized Drude conductivity [11, 12].

Recently, Ioffe and Millis suggested that the entire conductivity spectrum of the high- $T_c$  materials could be understood as a single component, rather than two, as in FLT [13]. The spectrum they derived was generalized by van der Marel to the following useful form [14],

$$\sigma(\omega) = \frac{A}{(1/\tau - i\omega)^\alpha}, \quad (1)$$

where  $A$  is a parameter with units that depend on the value of  $\alpha$ . Ioffe and Millis obtained  $\alpha = 1/2$  by assuming that the carrier lifetime depends strongly on its direction of motion [15, 16, 17, 18]. In the limit  $1/\tau \rightarrow 0$ , Eq. 1 is similar to one derived by Anderson [19], under different assumptions. Note that Eq. 1 includes the Drude form as a special case, with  $\alpha = 1$ . In allowing  $\alpha$  to deviate from unity, we obtain the observed power law dependence of the conductivity on frequency. However, we also subvert a standard assumption of transport physics, that the conductivity at  $\omega = 0$  is proportional to a scattering time. Instead, the dc conductivity is proportional to a fractional power of a scattering time, that is,  $\sigma_{dc} = A \tau^\alpha$ . Moreover, the analytical structure of  $\sigma(\omega)$  changes, from having a simple pole at  $\omega = -i/\tau$ , to being multiple-valued with a branch point there.

Although the models described above are distinct, they may be difficult to distinguish experimentally if the Drude component predicted by FLT is masked by the incoherent conductivity. The most stringent test of FLT is at low temperature, where the Drude component, if one exists, would be sharpest. In the cuprates, the temperature range over which the normal state conductivity can be studied is limited by the onset of superconductivity. The absence of superconductivity in  $\text{SrRuO}_3$  permits a much more meaningful test of FLT than previously available.

We find that  $\sigma(\omega, T)$  of  $\text{SrRuO}_3$  at low temperature is described well by Eq. 1 over nearly three decades in  $\omega$  ( $6\text{--}2400 \text{ cm}^{-1}$ ) with  $\alpha \sim 0.4$ , in strong disagreement with FLT. Our results at frequencies below  $100 \text{ cm}^{-1}$  were

obtained from transmission measurements on thin film samples of  $\text{SrRuO}_3$  grown epitaxially on  $\text{NdGaO}_3$  substrates [20, 21]. To probe the region where  $\omega \sim 1/\tau$ , we used conventional Fourier-transform infrared spectroscopy to measure the transmittance ( $\mathcal{T}$ ). For the range  $\omega \ll 1/\tau$ , we used time-domain terahertz spectroscopy (TDTHz) to measure the complex transmission amplitude  $t(\omega, T)$  in the millimeter wave region of the spectrum. The residual resistivity in these films is typically  $50 \mu\Omega\text{-cm}$ .  $\text{SrTiO}_3$  substrates produce  $\text{SrRuO}_3$  films with lower resistance, but this substrate material has such a large temperature-dependent dielectric constant that an accurate determination of the conductivity from transmission measurements is prohibitively difficult. At frequencies above  $100 \text{ cm}^{-1}$ , we measure the reflectivity from a thick film of  $\text{SrRuO}_3$  deposited on a  $\text{SrTiO}_3$  substrate [8]. We have derived  $\sigma(\omega, T)$  from each of these measurements, as described below.

We use TDTHz to measure the complex transmission amplitude  $t(\omega)$  of  $\text{SrRuO}_3$  in the range  $0.2\text{--}1.2 \text{ THz}$  ( $6\text{--}36 \text{ cm}^{-1}$ ) [22]. We compared the  $\text{SrRuO}_3$  film on its substrate to a bare  $\text{NdGaO}_3$  substrate at each temperature, using a vapor flow cryostat with a translating sample mount. The ratio of the two complex transmission amplitudes,  $t_{sr}(\omega) = t_{\text{sample}}(\omega)/t_{\text{ref}}(\omega)$ , is a simple function of the substrate index  $n$ ,  $\sigma(\omega)$  of the film, and the film thickness  $d$ :

$$t_{sr}(\omega) = \frac{n+1}{n+1+\sigma(\omega)Z_0d}. \quad (2)$$

$Z_0$  is the impedance of free space. We inverted Eq. 2 to obtain both the amplitude and phase of the complex conductivity as a function of temperature and frequency, which we show in Fig. 1 for our most thoroughly studied  $\text{SrRuO}_3$  film. Also shown are the results of the best fit to Eq. 1 with  $\alpha = 0.4$ , following the procedure described below. The statistical error on a typical measurement of the conductivity phase  $\phi_\sigma(\omega, T) = \arg[\sigma(\omega, T)]$  is  $\pm 0.02 \text{ rad}$  at  $1 \text{ THz}$ , two orders of magnitude better than that obtained in typical reflectivity measurements at this frequency. The temperature dependence of the effective path length in the substrate and cryostat windows provides the largest source of systematic error, which we estimate to be less than  $\pm 0.03 \text{ rad}$  at  $1 \text{ THz}$ . Errors in the measurement of the conductivity amplitude are dominated by statistical uncertainty in the transmission amplitude, which is typically  $\pm 3\%$ .

To obtain an objective best fit of Eq. 1 to the TDTHz measurements, we first perform a least-squares fit of the measured conductivity phase to  $\phi(\omega) = \alpha \tan^{-1}(\omega\tau)$  at each temperature, for several values of  $\alpha$ . This allows us to determine  $\tau(T; \alpha)$ , the best fit value of  $\tau$  for each temperature, with different assumed values of  $\alpha$ . Unlike a global fit to  $\sigma(\omega)$ , this procedure is independent of the conductivity amplitude. Next we performed a separate least-squares fit of the amplitude to  $|\sigma(\omega)| = A/(1/\tau^2 + \omega^2)^{\alpha/2}$ , using the  $\tau = \tau(T; \alpha)$  from the phase fits and allowing only  $A$  to vary. The quality of these fits [23] are

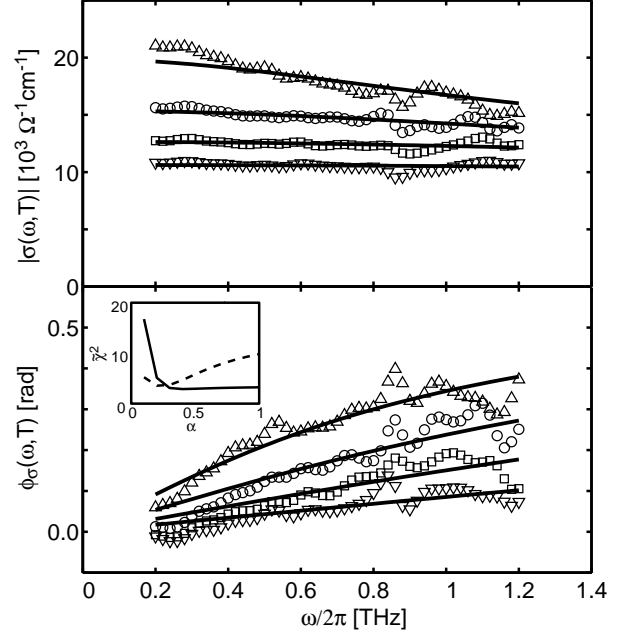


FIG. 1: Measured amplitude (upper panel) and phase (lower panel) of  $\sigma(\omega, T)$  in  $\text{SrRuO}_3$  at four representative temperatures.  $\triangle$ :  $T = 8 \text{ K}$ ,  $\circ$ :  $40 \text{ K}$ ,  $\square$ :  $60 \text{ K}$ , and  $\nabla$ :  $80 \text{ K}$ . Lines are fits to the data using Eq. 1, with  $\alpha = 0.4$ . The inset shows the reduced  $\chi^2$  error associated with the phase (solid line) and amplitude (dashed line) fits to Eq. 1, as a function of  $\alpha$ .

shown as a function of  $\alpha$  in the inset to Fig. 1. The phase fits exhibit a weak optimum at  $\alpha = 0.4$ , with a sharp decrease in quality below  $\alpha = 0.3$  but with relatively little change in quality as  $\alpha$  increases from 0.4 to unity. The amplitude fits, on the other hand, worsen dramatically as  $\alpha$  changes from 0.3 to unity. Taken together, these fits allow us to limit the range of acceptable values for  $\alpha$  to  $0.2\text{--}0.5$ .

We develop this analysis further in Fig. 2, which shows a logarithmic plot of the conductivity amplitude at our lowest frequency,  $\omega_1/2\pi = 0.2 \text{ THz}$ , versus  $[\tau(T; \alpha)]^\alpha$ , with  $\tau$  in femtoseconds. The plot is parametric in temperature for several different values of  $\alpha$ . In Eq. 1,  $\sigma(\omega \rightarrow 0) = A\tau^\alpha$ ; if  $A$  remains constant with temperature, Eq. 1 will yield a straight line with unity slope on this plot, indicated by the dotted line. The best fit to this slope is obtained for  $\alpha = 0.4$ , and already at  $\alpha = 0.6$  a clear deviation is observed. At higher values of  $\alpha$  the slope decreases yet further, so the case  $\alpha = 1$  corresponding to Drude conductivity requires  $A$  to increase strongly with temperature. Thus,  $\alpha = 0.4 \pm .1$  provides not only the best fit to Eq. 1, but also the most compact description of the data.

In Fig. 3 we show  $\sigma_1(\omega)$  of  $\text{SrRuO}_3$  over two and a half decades in frequency, obtained in three separate measurements. Data in the lowest frequency range is taken from TDTHz measurements at the same four represen-

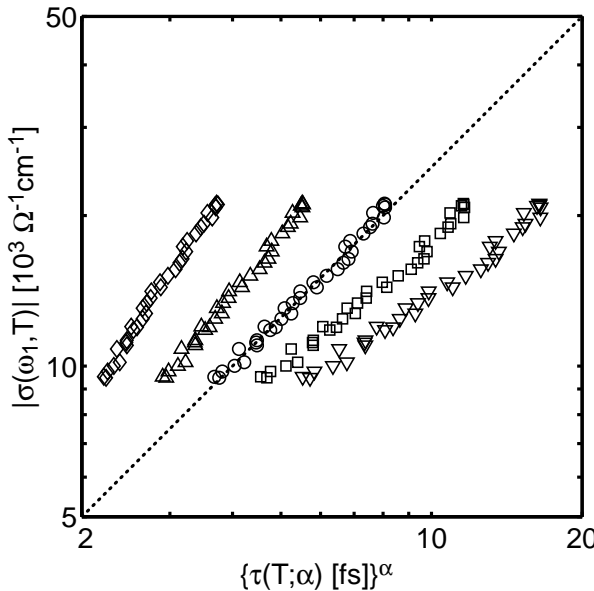


FIG. 2: Logarithmic plot demonstrating the scaling relationship of  $\sigma(\omega_1, T)$ ,  $\omega_1/2\pi = 0.2$  THz, and  $\tau(T; \alpha)$  obtained by fitting to Eq. 1. The plot is parametric in temperature from 5–92.5 K in steps of 2.5 K, for various choices of  $\alpha$ :  $\diamond$ , 0.2;  $\triangle$ , 0.3;  $\circ$ , 0.4;  $\square$ , 0.5; and  $\nabla$ , 0.6. The dotted line is given by  $\sigma(\omega = 0) \propto \tau^\alpha$ .

tative temperatures shown in Fig. 1, and extends from 6–36 cm<sup>-1</sup>. In the intermediate frequency range 26–80 cm<sup>-1</sup>, we have measured  $\mathcal{T}(\omega, T)$ , which is a real quantity and therefore incapable of providing the complex conductivity without further analysis. Using the  $\tau(T)$  obtained from TDTHz for  $\alpha = 0.4$ , we have calculated the conductivity phase expected in this frequency range at each temperature, then used these phase values to calculate the conductivity amplitude directly from  $\mathcal{T}(\omega, T)$ . The results of this procedure are shown for the same four temperatures as the TDTHz data. The continuity of the results at the crossover frequency of these two distinct measurements may be taken as an indication of the high accuracy with which we have determined the conductivity. At frequencies probed by infrared reflectivity, the conductivity is relatively temperature independent below 100 K, and we show only one measurement taken at 40 K [8].

With the parameters obtained from the TDTHz data, Eq. 1 may be used to predict the behavior of the conductivity at all frequencies and temperatures. The dotted lines in Fig. 3 show the conductivity calculated from Eq. 1, using the parameters obtained from TDTHz. With a single global parameter  $A$  and a single temperature-dependent parameter  $\tau(T)$ , this model fits the data exceptionally well, at frequencies two orders of magnitude higher than those at which the parameters were obtained. As we increase the temperature above 95 K, both our measurements and earlier reflectivity measurements begin to deviate from the form discussed here, and develop

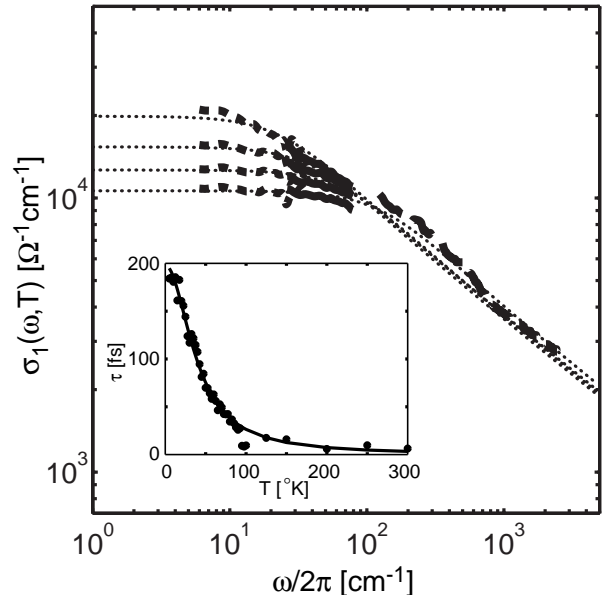


FIG. 3: Logarithmic plot of the conductivity obtained by three methods, in three ranges of frequency. The conductivity obtained from the infrared reflectivity at 40 K is indicated by the long dashed line. Results from far-infrared transmission measurements, as described in the text, are indicated by solid lines, and TDTHz measurements by short dashed lines, with both sets ordered in temperature from top to bottom with  $T = 8$  K, 40 K, 60 K, and 80 K. Least-squared fits to Eq. 1 using only TDTHz data are shown by dashed lines. Inset: temperature dependence of  $\tau$  obtained for  $\alpha = 0.4$  (closed circles), compared to Eq. 3 (solid line).

a pseudogap structure which may be related to the transition from ferromagnetism to paramagnetism [8]. We leave a detailed discussion of this behavior to a later publication, limiting our discussion here to temperatures below 95 K, deep within the ferromagnetic state.

As shown in Fig. 3,  $1/\tau$  sets the frequency scale at which the  $\omega^{-\alpha}$  divergence is cut off, forcing  $\sigma_1 \propto \tau^\alpha$  in the dc limit. Thus the ubiquitous practice of inferring scattering times from electrical transport via  $\sigma_{dc} \propto \tau$  is erroneous, whenever the conductivity behaves as Eq. 1 with  $\alpha \neq 1$ . The resistivity of SrRuO<sub>3</sub> for  $25 \text{ K} \lesssim T \lesssim 120 \text{ K}$  exhibits approximately linear temperature dependence, which then crosses over at lower temperatures to become constant as impurity scattering dominates [7]. In our analysis, this implies a scattering rate with at least a quadratic dependence on temperature.

A simple form which approximates the observed behavior is

$$\frac{\hbar}{\tau(T)} = \frac{\hbar}{\tau_0} + \frac{k_B T^2}{T_0}, \quad (3)$$

with a temperature independent, or elastic, scattering time  $\tau_0$  and a characteristic temperature  $T_0$  [13]. Here,  $\hbar$  is Planck's constant, and  $k_B$  Boltzmann's constant.

This gives a temperature dependent resistivity,  $\rho(T) = A + BT^2$ , observed in the highest quality films at low temperatures [24]. The inset to Fig. 3 shows  $\tau(T; 0.4)$  together with the best fit to Eq. 3, with  $\tau_0 = 198$  fs and  $T_0 = 40$  K. The agreement is quite good over the entire temperature range, although in the region  $T > 95$  K  $\tau$  is comparable to our measurement accuracy.

It is interesting to note that despite the discrepancy of Eq. 1 with FLT, the functional form of Eq. 3 is exactly what FLT would predict for  $\tau$ , though with  $T_0$  at least two orders of magnitude larger than 40 K. The origin of this temperature dependence, and of the low energy scale  $T_0$  which controls it, remains one of the important open questions raised by these measurements. Similar behavior has recently been observed in the normal state of  $\text{Bi}_2\text{Sr}_2\text{CaCu}_2\text{O}_8$  [25], and we expect that a considerable body of transport work will require reanalysis in light of the observations presented here. For example, Shubnikov-de Haas oscillations have been observed in  $\text{SrRuO}_3$ , with amplitudes that display the temperature dependence of a Fermi liquid [24]. It would be interesting to develop theories which produce Eq. 1, to address the existence of these quantum oscillations.

In summary, we have studied in detail the complex conductivity of  $\text{SrRuO}_3$  at low frequencies and temperatures, and shown that it agrees well with the simple phenomenological form given in Eq. 1. The difference between  $\alpha \sim 0.4$  observed here and the Drude form expected from FLT, with  $\alpha = 1$ , is reflected in the interpretation of  $\tau$ , one of the fundamental parameters in the transport theory of metals. We have described how this quantity influences the measured conductivity, but proper interpretation of its microscopic meaning must await further analysis. In particular, careful studies of the dependence of  $\tau$  on substitutional impurities or structural disorder would help to reveal its physical origin [13].

J. S. D. thanks Daniel Chemla for encouragement in pursuing this work. This work was supported by the Director, Office of Energy Research, Office of Basic Energy Sciences, Division of Materials Sciences of the U. S. Department of Energy under Contract No. DE-AC03-76SF00098, by the Stanford NSF-MRSEC Program, and by NSF grants DMR-0071949 and 9870252.

- [1] P. W. Anderson, *Science* **235**, 1196 (1987).
- [2] D. Pines and P. Nozières, *The Theory of Quantum*

*Liquids, Vol. 1: Normal Fermi Liquids* (Addison-Wesley, 1989).

- [3] J. Orenstein and A. J. Millis, *Science* **288**, 468 (2000).
- [4] M. Imada, A. Fujimori, and Y. Tokura, *Rev. Mod. Phys.* **70**, 1039 (1998).
- [5] I. Bozovic *et al.*, *Phys. Rev. Lett.* **73**, 1436 (1994).
- [6] L. Klein *et al.*, *Phys. Rev. Lett.* **77**, 2774 (1996).
- [7] L. Klein *et al.*, *J. Phys.: Condens. Matter* **8**, 10111 (1996).
- [8] P. Kostic *et al.*, *Phys. Rev. Lett.* **81**, 2498 (1998).
- [9] Z. Schlesinger *et al.*, *Phys. Rev. Lett.* **65**, 801 (1990).
- [10] A. E. Azrak *et al.*, *Phys. Rev. B* **49**, 9846 (1994).
- [11] D. B. Tanner and T. Timusk, in *Physical Properties of High Temperature Superconductors III*, edited by D. M. Ginsberg (World Scientific, Singapore, 1992), pp. 363–469.
- [12] A. Georges *et al.*, *Rev. Mod. Phys.* **68**, 13 (1996).
- [13] L. B. Ioffe and A. J. Millis, *Phys. Rev. B* **58**, 11631 (1998).
- [14] D. van der Marel, *Phys. Rev. B* **60**, R765 (1999).
- [15] A. Carrington *et al.*, *Phys. Rev. Lett.* **69**, 2855 (1992).
- [16] R. Hlubina and T. M. Rice, *Phys. Rev. B* **51**, 9253 (1995).
- [17] B. Stojković and D. Pines, *Phys. Rev. Lett.* **76**, 811 (1996).
- [18] T. Xiang and W. N. Hardy, *cond-mat/0001443*.
- [19] P. W. Anderson, *Phys. Rev. B* **55**, 11785 (1997).
- [20] C. H. S. Ahn, Ph.D. thesis, Stanford University (1996).
- [21] C. B. Eom *et al.*, *Science* **258**, 1766 (1992).
- [22] M. C. Nuss and J. Orenstein, in *Millimeter and Submillimeter Wave Spectroscopy of Solids*, edited by G. Grüner (Springer, Berlin, 1998), vol. 74 of *Topics in Applied Physics*, pp. 7–50.
- [23] The reduced  $\chi^2$  values shown are obtained by fixing  $\alpha$ , finding the  $\chi^2$  error on fits to Eq. 1 for all temperatures from 5–92.5 K and all frequencies from 0.2–1.2 THz, then dividing by the total number of degrees of freedom, equal to the number of data points minus the number of free parameters in the fit.
- [24] A. P. Mackenzie *et al.*, *Phys. Rev. B* **58**, R13318 (1998).
- [25] J. Corson *et al.*, *cond-mat/0006027*.